

Transverse spin with high energy polarized beams in a collider

Alexei Prokudin



EIC collaboration meeting
Stony Brook , January 10 – 12, 2010



Introduction

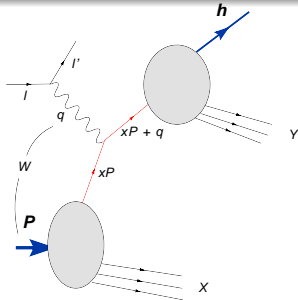
The biggest Single Spin Asymmetries ($\sim 40\%$) were measured in $P^\uparrow P \rightarrow \pi X$. They were thought to be *negligible* due to “simple” arguments of helicity conservation in QED and QCD interactions, thus $A_N \sim \alpha_s \frac{m_q}{P_T}$. Nevertheless *experimental* measurements proved this prediction to be wrong.

$\langle \cos\phi \rangle$ asymmetry in unpolarised SIDIS was proposed as a “*clean test of perturbative QCD*” and again *experimental* measurements revealed that such an asymmetry carries information on intrinsic motion of partons inside the proton.

Experiments with polarized targets were always source of new information about partonic structure of hadrons and frequently changed our understanding of parton dynamics.

Future experimental measurements at EIC will bring us valuable information on the structure of the proton and on the validity of our current theoretical framework.

Semi Inclusive Deep Inelastic Scattering



Kinematical variables:

$$Q^2 = -q^2,$$

$$x_{Bj} = \frac{Q^2}{2P \cdot q},$$

$$y = \frac{Q^2}{(s - m_p^2)x_{Bj}},$$

$$z = \frac{P \cdot h}{P \cdot q},$$

$$W^2 = Q^2 \frac{1-x_{Bj}}{x_{Bj}} + m_p^2$$

Cross section

$$d\sigma \equiv \frac{d^5 \sigma^{\ell p \rightarrow \ell' h X}}{dx_{Bj} dy dz_h d^2 \mathbf{P}_T} \propto L_{\mu\nu} W^{\mu\nu}$$

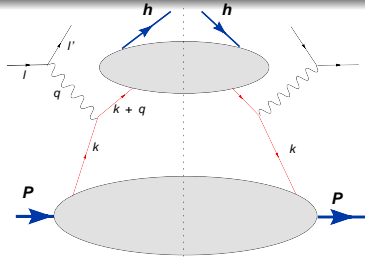
Leptonic tensor

$$L_{\mu\nu} = 2(l_\mu l'_\nu + l'_\nu l_\mu - l \cdot l' g_{\mu\nu}) + 2i\lambda_e \epsilon_{\mu\nu\rho\sigma} l^\rho l'^\sigma$$

Hadronic tensor

$$W^{\mu\nu} \propto \sum_X \int \frac{d^3 \mathbf{P}_X}{2P_X^0} \delta^{(4)}(q + P - P_X - P_h) \langle PS | J^\mu(0) | h, X \rangle \langle h, X | J^\nu(0) | PS \rangle$$

TMD Factorization in Semi Inclusive Deep Inelastic Scattering

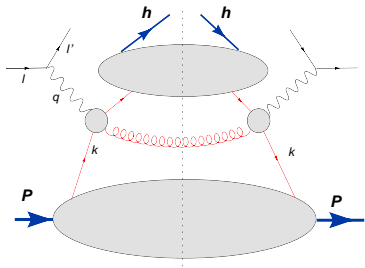


Cross section

$$d\sigma \propto L_{\mu\nu} W^{\mu\nu} = \sum_q \int d^2\mathbf{k}_\perp d^2\mathbf{p}_\perp f_{q/p}(x, \mathbf{k}_\perp, \dots) \otimes \sigma \otimes D_q^h(z, \mathbf{p}_\perp, \dots)$$

Intrinsic transverse momenta \mathbf{k}_\perp and \mathbf{p}_\perp are of non perturbative origin. Polarised case is explored in TMD factorization formalism Kotzinian 1995; Mulders, Tangerman 1995; Goeke, Metz, Schlegel 2005, Bacchetta et al 2007

Collinear Factorization in Semi Inclusive Deep Inelastic Scattering



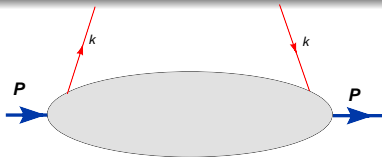
Collinear factorization Collins, Soffer, Sterman 1982, Meng, Olness, Soper 1996 is valid for hard $P_T \sim Q \gg \Lambda_{QCD}$ and describes SIDIS cross section as convolution of usual integrated distribution and fragmentation functions. Gluon radiation generates P_T of the produced hadron.

Cross section

$$d\sigma \propto L_{\mu\nu} W^{\mu\nu} = \sum_q \int f_{q/p}(x, \dots) \otimes \sigma \otimes D_q^h(z, \dots)$$

In polarized case multi-parton correlations play role in collinear factorization formalism Efremov, Teryaev 1982; Qiu, Sterman 1991; Ji, Qui, Vogelsang, Yuan 2006.

Quark-quark Correlator



$$\Phi_{ij}(P, k, S) = \int \frac{d^4\xi}{(2\pi)^4} e^{ik \cdot \xi} \langle P, S | \bar{\psi}_j(0) \mathcal{W}(0, \xi | n_-) \psi_j(\xi) | P, S \rangle$$

Mulders, Tangerman 1995; Goeke, Metz, Schlegel 2005, Bacchetta et al 2007

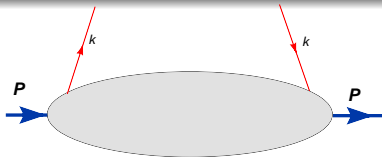
Gauge link $\mathcal{W}(0, \xi | n_-)$ ensures gauge invariance of the correlator.
TMD distribution functions can be found via k^- integration

$$\Phi(P, k_\perp, S) = \int dk^- \Phi(P, k, S)$$

Dirac decomposition is done by

$$\Phi^{[\Gamma]}(P, k_\perp, S) = \frac{1}{2} \text{Tr}(\Phi(P, k_\perp, S) \Gamma)$$

Quark-quark Correlator



$$\Phi_{ij}(P, k, S) = \int \frac{d^4\xi}{(2\pi)^4} e^{ik\cdot\xi} \langle P, S | \bar{\psi}_j(0) \mathcal{W}(0, \xi | n_-) \psi_j(\xi) | P, S \rangle$$

Mulders, Tangerman 1995; Goeke, Metz, Schlegel 2005, Bacchetta et al 2007

Twist-2 decomposition contains **8 functions**:

$$\Phi^{[\gamma^+]}(P, k_\perp, S) = f_1(x, k_\perp^2) - \frac{\epsilon_T^{ij} k_{\perp i} S_{Tj}}{M} f_{1T}^\perp(x, k_\perp^2)$$

$$\Phi^{[\gamma^+ \gamma_5]}(P, k_\perp, S) = S_L g_{1L}(x, k_\perp^2) - \frac{k_\perp \cdot S_T}{M} g_{1T}^\perp(x, k_\perp^2)$$

$$\Phi^{[i\sigma^{i+} \gamma_5]}(P, k_\perp, S) = S_T^i h_1 + S_L \frac{k_\perp^i}{M} h_{1L}^\perp - \frac{k_\perp^i k_\perp^j - 1/2 k_\perp^2 g_T^{ij}}{M^2} S_{Tj} h_{1T}^\perp - \frac{\epsilon_T^{ij} k_{\perp j}}{M} h_1^\perp$$

"Amsterdam notation" is used for the TMDs

Parton distribution functions

- Collinear Parton Distribution Functions:

$$f_{a/A}(x_a), \underbrace{\Delta q(x_a)}_{g_1}, \underbrace{\Delta_T q(x_a)}_{\text{Transversity } h_1}$$

- Transverse Momentum Dependent (TMD) PDFs

Kotzinian 1995; Mulders, Tangerman 1995; Bacchetta et al 07; Anselmino et al 06

① Hadron A unpolarized: $\hat{f}_{a/A}(x_a, k_{\perp a})$, $\underbrace{\Delta \hat{f}_{s_y/A}(x_a, k_{\perp a})}_{\text{Boer-Mulders}} h_1^\perp$

② Transversely polarised hadron A^\uparrow :

$$\underbrace{\Delta \hat{f}_{a/A^\uparrow}(x_a, k_{\perp a})}_{\text{Sivers}} f_{1T}^\perp, \underbrace{\Delta \hat{f}_{s_x/A^\uparrow}^q(x_a, k_{\perp a}), \Delta^- \hat{f}_{s_y/A^\uparrow}(x_a, k_{\perp a})}_{\text{Transversity}} h_1, h_{1T}^\perp$$

$$\underbrace{\Delta \hat{f}_{s_z/A^\uparrow}(x_a, k_{\perp a})}_{g_{1T}^\perp}$$

③ Longitudinally polarized hadron A^\rightarrow :

$$\underbrace{\Delta \hat{f}_{s_z/+}(x_a, k_{\perp a})}_{\Delta q}, \underbrace{\Delta \hat{f}_{s_x/+}(x_a, k_{\perp a})}_{h_{1L}^\perp}$$

Parton distribution functions

- Collinear Parton Distribution Functions:

$$f_{a/A}(x_a), \underbrace{\Delta q(x_a)}_{g_1}, \underbrace{\Delta_T q(x_a)}_{\text{Transversity } h_1}$$

- Transverse Momentum Dependent (TMD) PDFs

Kotzinian 1995; Mulders, Tangerman 1995; Bacchetta et al 07; Anselmino et al 06

- ➊ Hadron A unpolarized: $\hat{f}_{a/A}(x_a, k_{\perp a})$, $\underbrace{\Delta \hat{f}_{s_y/A}(x_a, \mathbf{k}_{\perp a})}_{\text{Boer-Mulders}} h_1^{\perp}$

- ➋ Transversely polarised hadron A^{\uparrow} :

$$\underbrace{\Delta \hat{f}_{a/A^{\uparrow}}(x_a, \mathbf{k}_{\perp a})}_{\text{Sivers}} f_{1T}^{\perp}, \underbrace{\Delta \hat{f}_{s_x/A^{\uparrow}}^q(x_a, \mathbf{k}_{\perp a}), \Delta^- \hat{f}_{s_y/A^{\uparrow}}(x_a, \mathbf{k}_{\perp a})}_{\text{Transversity}} h_1, h_{1T}^{\perp}$$

$$\underbrace{\Delta \hat{f}_{s_z/A^{\uparrow}}(x_a, \mathbf{k}_{\perp a})}_{g_{1T}^{\perp}}$$

- ➌ Longitudinally polarized hadron A^{\rightarrow} :

$$\underbrace{\Delta \hat{f}_{s_z/+}(x_a, \mathbf{k}_{\perp a})}_{\Delta q}, \underbrace{\Delta \hat{f}_{s_x/+}(x_a, \mathbf{k}_{\perp a})}_{h_{1L}^{\perp}}$$

Parton distribution functions

- Collinear Parton Distribution Functions:

$$f_{a/A}(x_a), \underbrace{\Delta q(x_a)}_{g_1}, \underbrace{\Delta_T q(x_a)}_{\text{Transversity } h_1}$$

- Transverse Momentum Dependent (TMD) PDFs

Kotzinian 1995; Mulders, Tangerman 1995; Bacchetta et al 07; Anselmino et al 06

- ① Hadron A unpolarized: $\hat{f}_{a/A}(x_a, k_{\perp a})$, $\underbrace{\Delta \hat{f}_{s_y/A}(x_a, \mathbf{k}_{\perp a})}_{\text{Boer-Mulders}} h_1^{\perp}$

- ② Transversely polarised hadron A^{\uparrow} :

$$\underbrace{\Delta \hat{f}_{a/A^{\uparrow}}(x_a, \mathbf{k}_{\perp a})}_{\text{Sivers}} f_{1T}^{\perp}, \underbrace{\Delta \hat{f}_{s_x/A^{\uparrow}}^q(x_a, \mathbf{k}_{\perp a}), \Delta^- \hat{f}_{s_y/A^{\uparrow}}(x_a, \mathbf{k}_{\perp a})}_{\text{Transversity}} h_1, h_{1T}^{\perp}$$

$$\underbrace{\Delta \hat{f}_{s_z/A^{\uparrow}}(x_a, \mathbf{k}_{\perp a})}_{g_{1T}^{\perp}}$$

- ③ Longitudinally polarized hadron A^{\rightarrow} :

$$\underbrace{\Delta \hat{f}_{s_z/+}(x_a, \mathbf{k}_{\perp a})}_{\Delta q}, \underbrace{\Delta \hat{f}_{s_x/+}(x_a, \mathbf{k}_{\perp a})}_{h_{1L}^{\perp}}$$

Parton distribution functions

- Collinear Parton Distribution Functions:

$$f_{a/A}(x_a), \underbrace{\Delta q(x_a)}_{g_1}, \underbrace{\Delta_T q(x_a)}_{\text{Transversity } h_1}$$

- Transverse Momentum Dependent (TMD) PDFs

Kotzinian 1995; Mulders, Tangerman 1995; Bacchetta et al 07; Anselmino et al 06

- ① Hadron A unpolarized: $\hat{f}_{a/A}(x_a, k_{\perp a})$, $\underbrace{\Delta \hat{f}_{s_y/A}(x_a, \mathbf{k}_{\perp a})}_{\text{Boer-Mulders}} h_1^{\perp}$

- ② Transversely polarised hadron A^{\uparrow} :

$$\underbrace{\Delta \hat{f}_{a/A^{\uparrow}}(x_a, \mathbf{k}_{\perp a})}_{\text{Sivers}} f_{1T}^{\perp}, \underbrace{\Delta \hat{f}_{s_x/A^{\uparrow}}^q(x_a, \mathbf{k}_{\perp a}), \Delta^- \hat{f}_{s_y/A^{\uparrow}}(x_a, \mathbf{k}_{\perp a})}_{\text{Transversity}} h_1, h_{1T}^{\perp}$$

$$\underbrace{\Delta \hat{f}_{s_z/A^{\uparrow}}(x_a, \mathbf{k}_{\perp a})}_{g_{1T}^{\perp}}$$

- ③ Longitudinally polarized hadron A^{\rightarrow} :

$$\underbrace{\Delta \hat{f}_{s_z/+}(x_a, \mathbf{k}_{\perp a})}_{\Delta q}, \underbrace{\Delta \hat{f}_{s_x/+}(x_a, \mathbf{k}_{\perp a})}_{h_{1L}^{\perp}}$$

Electron Ion Collider

- Electron Ion Collider project is proposed to study Polarized SIDIS at the medium – high energies $200 \leq s \leq 3000$ GeV 2 thus providing a big span in $1 \leq Q^2 \leq 100$ GeV 2 and $0 \leq P_T \leq 3$ GeV.
- Complete spin and flavour decomposition is possible both in valence and sea-quark region, $x_{min} \sim 10^{-3} \div 10^{-4}$.
- Possibility of high Q^2 range and level arm allows to study twist-2 functions and higher twist content of the nucleon.
- Range of P_T allows to study intermediate region where both TMD and collinear factorizations are valid.
- Changing Q^2 at some fixed x provides information on Q^2 behaviour of the asymmetries and Q^2 evolution of TMDs.

TMDs and Structure functions Unpolarised hadron

$$F_{UU} = f_1 \otimes D_1$$

$$F_{UU}^{\cos \phi_h} = \frac{1}{Q} (f_1 \otimes D_1 + h_1^\perp \otimes H_1^\perp + \dots)$$

$$F_{UU}^{\cos 2\phi_h} = \underbrace{h_1^\perp}_{\text{Boer-Mulders}} \otimes \underbrace{H_1^\perp}_{\text{Collins FF}}$$

$$F_{AB}^{\sin(\cos)\phi_x}$$

beam polarization $A = U, L$,
hadron polarization $B = U, L, T$
and contribution to cross
section

$$\sigma \propto \sin(\cos)\phi_x \cdot F_{AB}^{\sin(\cos)\phi_x}$$

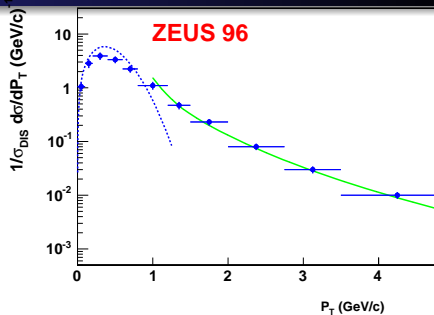
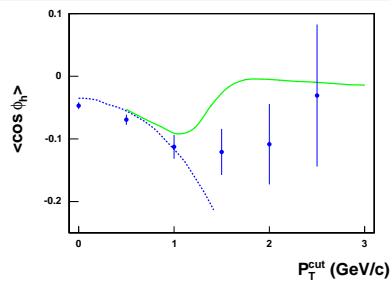
Boer-Mulders distribution (Boer and Mulders 1998) describes distribution of transversely polarised quarks in unpolarised hadron.

Measuring F_{UU} we access non perturbative dynamics of parton motion.
Intermediate $P_T \rightarrow$ both TMD and Collinear factorizations are valid.

Using a simple gaussian approximation we can obtain widths $\langle k_\perp^2 \rangle = 0.25$ GeV 2 $\langle p_\perp^2 \rangle = 0.2$ GeV 2 (Anselmino et al 2007) of f_1 and D_1

Where are some hints that $\langle k_\perp^2 \rangle_u \neq \langle k_\perp^2 \rangle_d$ and on x and z dependence of $\langle k_\perp^2 \rangle$ and $\langle p_\perp^2 \rangle$.

From low to high P_T Anselmino et al 2007



TMD σ_0 and collinear QCD σ_1 cross sections are included:

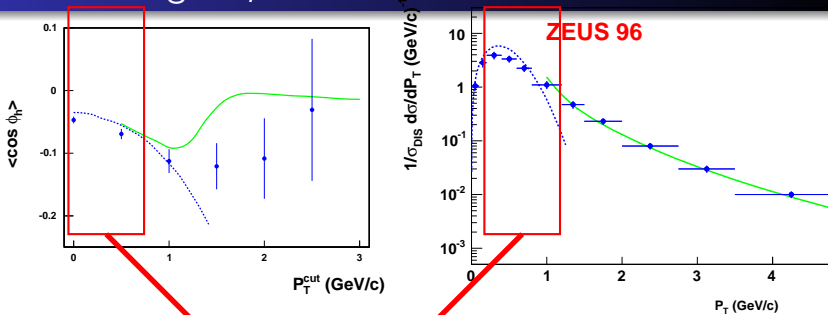
$$d\sigma = \alpha_s^0 d\sigma_0 + \alpha_s^1 d\sigma_1 + \alpha_s^2 d\sigma_2 \simeq \\ \alpha_s^0 d\sigma_0 + K \alpha_s^1 d\sigma_1$$

$K \simeq 1.5$, The data are from **ZEUS** and **E665**.

Fermilab E665 Collaboration, M.R. Adams *et al.*, *Phys. Rev.* **D48** (1993) 5057.

M. Derrick *et al.*, ZEUS Collaboration, *Z. Phys.* **C70** (1996) 1.

From low to high P_T Anselmino et al 2007



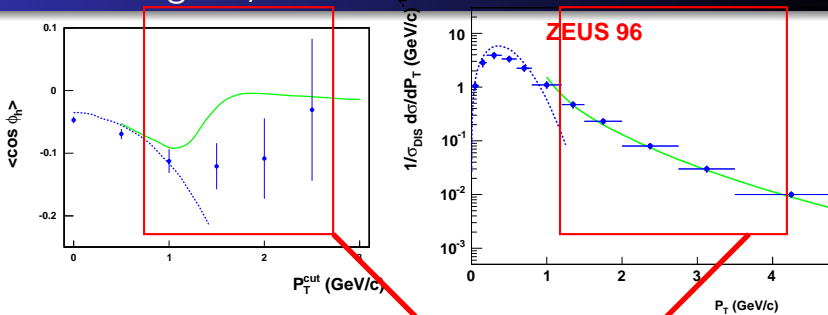
TMD σ_0 and collinear QCD σ_1 cross sections are included:

$$d\sigma = \alpha_s^0 d\sigma_0 + \alpha_s^1 d\sigma_1 + \alpha_s^2 d\sigma_2 \simeq \\ \alpha_s^0 d\sigma_0 + K \alpha_s^1 d\sigma_1$$

$$\langle k_\perp^2 \rangle = 0.25 \text{ GeV}^2 \quad \langle p_\perp^2 \rangle = 0.2 \text{ GeV}^2$$

in accordance with lattice results Musch et al, 2008

From low to high P_T Anselmino et al 2007



TMD σ_0 and collinear QCD σ_1 cross sections are included.

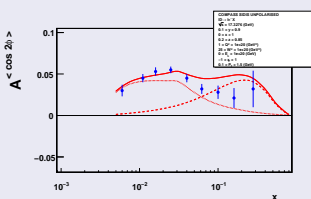
$$d\sigma = \alpha_s^0 d\sigma_0 + \alpha_s^1 d\sigma_1 + \alpha_s^2 d\sigma_2 \simeq \\ \alpha_s^0 d\sigma_0 + K \alpha_s^1 d\sigma_1$$

$$\langle k_\perp^2 \rangle = 0.25 \text{ GeV}^2 \quad \langle p_\perp^2 \rangle = 0.2 \text{ GeV}^2$$

in accordance with lattice results Musch et al, 2008

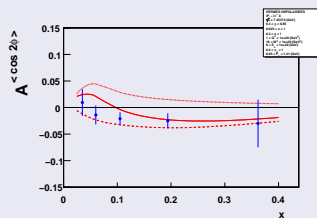
Boer-Mulders data

COMPASS $A_{UU}^{\cos 2\phi_h}$



Barone, Melis, AP arXiv:0912.5194

HERMES $A_{UU}^{\cos 2\phi_h}$



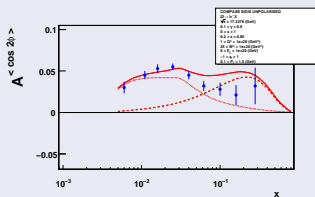
Barone, Melis, AP arXiv:0912.5194

$$F_{UU}^{\cos 2\phi_S} = h_1^\perp \otimes H_1^\perp + \frac{1}{Q^2} f_1 \otimes D_1$$

Twist-2 contribution (the dashed line) is comparable to higher twist (the dotted line) contribution at low Q^2 . EIC at high Q^2 allows to measure $h_1^\perp \otimes H_1^\perp$ without higher twists.

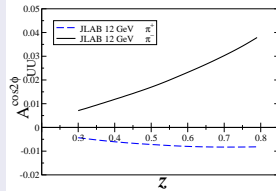
Boer-Mulders data

COMPASS $A_{UU}^{\cos 2\phi_h}$



Barone, Melis, AP arXiv:0912.5194

JLAB $A_{UU}^{\cos 2\phi_h}$



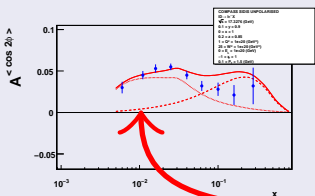
Gamberg, Goldstein, Schlegel,
 Phys.Rev.D77:094016,2008

$$F_{UU}^{\cos 2\phi_S} = h_1^\perp \otimes H_1^\perp + \frac{1}{Q^2} f_1 \otimes D_1$$

Twist-2 contribution (the dashed line) is comparable to higher twist (the dotted line) contribution at low Q^2 . EIC at high Q^2 allows to measure $h_1^\perp \otimes H_1^\perp$ without higher twists.

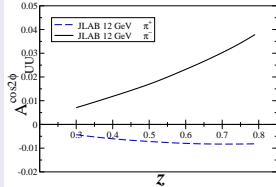
Boer-Mulders data

COMPASS $A_{UU}^{\cos 2\phi_h}$



Barone, Melis, AP arXiv:0912.5194

JLAB $A_{UU}^{\cos 2\phi_h}$



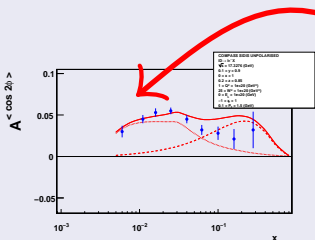
Gamberg, Goldstein, Schlegel,
Phys.Rev.D77:094016,2008

$$F_{UU}^{\cos 2\phi_S} = h_1^\perp \otimes H_1^\perp + \frac{1}{Q^2} f_1 \otimes D_1$$

Twist-2 contribution (the dashed line) is comparable to higher twist (the dotted line) contribution at low Q^2 . EIC at high Q^2 allows to measure $h_1^\perp \otimes H_1^\perp$ without higher twists.

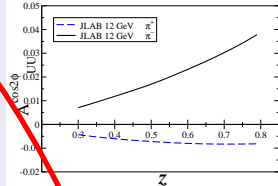
Boer-Mulders data

COMPASS $A_{UU}^{\cos 2\phi_h}$



Barone, Melis, AP arXiv:0912.5194

JLAB $A_{UU}^{\cos 2\phi_h}$



Gamberg, Goldstein, Schlegel,
Phys.Rev.D77:094016,2008

$$F_{UU}^{\cos 2\phi_S} = h_1^\perp \otimes H_1^\perp + \frac{1}{Q^2} f_1 \otimes D_1$$

Twist-2 contribution (the dashed line) is comparable to higher twist (the dotted line) contribution at low Q^2 . EIC at high Q^2 allows to measure $h_1^\perp \otimes H_1^\perp$ without higher twists.

TMDs: Longitudinally polarized hadron

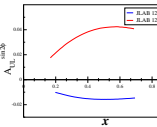
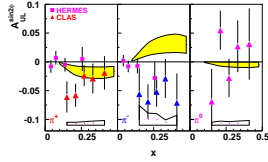
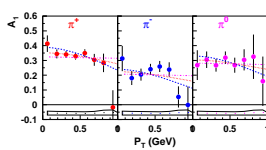
$$F_{LL} = g_{1L} \otimes D_1$$

$$F_{UL}^{\sin 2\phi_h} = h_{1L}^\perp \otimes H_1^\perp$$

h_{1L}^\perp describes distribution of transversely polarized quarks in longitudinally polarized hadron.

g_{1L} can be accessed at low x . Study of k_\perp dependence of g_{1L} is possible. Is its width equal to that of f_1 ?

HERMES, JLab and COMPASS measure $F_{UL}^{\sin 2\phi_h}$ and F_{LL}



data: HERMES, Airapetian et al 00, JLab, Avakian et al 2009, theory: Anselmino et al 07, Boffi et al 09, Gamberg et al 08

TMDs: Transversely polarized hadron

$$F_{UT}^{\sin(\phi_h - \phi_s)} = f_{1T}^\perp \otimes D_1 \quad \text{Sivers effect}$$

$$F_{UT}^{\sin(\phi_h + \phi_s)} = h_1 \otimes H_1^\perp \quad \text{Collins effect}$$

$$F_{UT}^{\sin(3\phi_h - \phi_s)} = h_{1T}^\perp \otimes H_1^\perp \quad F_{LT}^{\cos(\phi_h - \phi_s)} = g_{1T}^\perp \otimes D_1$$

Sivers function f_{1T}^\perp describes distribution of unpolarised quarks in transversely polarized hadron.

Transversity h_1 describes distribution of transversely polarized quarks in transversely polarized hadron. Survives k_\perp integration.

h_{1T}^\perp describes distribution of transversely polarized quarks in transversely polarized hadron, vanishes under k_\perp integration. $h_{1T}^\perp = g_1 - h_1$ in some models. Some preliminary data are available from HERMES and COMPASS.

g_{1T}^\perp describes distribution of longitudinally polarized quarks in a transversely polarized hadron. *No experimental data are available!*

Sivers effect

The azimuthal asymmetry $A_{UT}^{\sin(\phi_h - \phi_S)}$ arises due to Sivers function

$$f_{q/p^\dagger}(x, \mathbf{k}_\perp) = f_{q/p}(x, \mathbf{k}_\perp) + \frac{1}{2} \Delta^N f_{q/p^\dagger}(x, \mathbf{k}_\perp) \mathbf{S}_T \cdot (\hat{\mathbf{P}} \times \hat{\mathbf{k}}_\perp)$$

Sivers 90

$$A_{UT}^{\sin(\phi_H - \phi_S)} \sim \Delta^N f_{q/p^\dagger}(x, k_\perp) \otimes D_{h/q}(z, p_\perp)$$

$\mathbf{S}_T \cdot (\hat{\mathbf{P}} \times \hat{\mathbf{k}}_\perp)$ – correlation between the spin and angular momentum implies non zero contribution $\langle L_z^{q,\bar{q}} \rangle \neq 0$

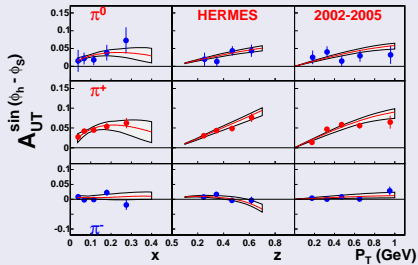
Data are available from HERMES and COMPASS.

First hints on nonzero sea quark Sivers functions.

HERMES and COMPASS DATA

HERMES

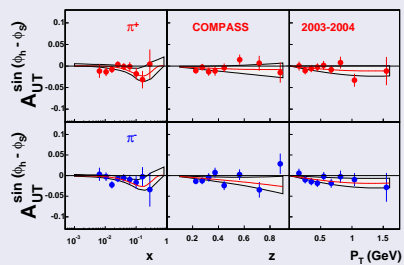
$ep \rightarrow e\pi X$, $p_{lab} = 27.57$ GeV.



M. Anselmino et al 2009

COMPASS

$\mu D \rightarrow \mu\pi X$, $p_{lab} = 160$ GeV.



M. Anselmino et al 2009

$$lp^\uparrow \rightarrow l\pi^+ X \simeq \Delta^N u \otimes D_{u/\pi^+} > 0$$

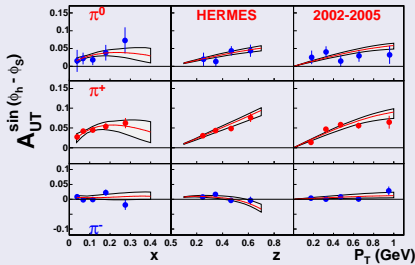
$$lp^\uparrow \rightarrow l\pi^- X \simeq 4\Delta^N u \otimes D_{u/\pi^-} + \Delta^N d \otimes D_{d/\pi^-} \simeq 0$$

$$ID^\uparrow \rightarrow l\pi^+ X \simeq (\Delta^N u + \Delta^N d) \otimes D_{u/\pi^+} \simeq 0$$

HERMES and COMPASS DATA

HERMES

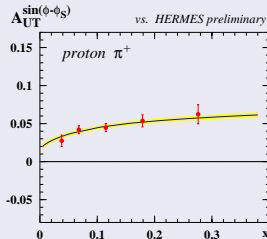
$ep \rightarrow e\pi X, p_{lab} = 27.57 \text{ GeV.}$



M. Anselmino et al 2009

HERMES

$ep \rightarrow e\pi X, p_{lab} = 27.57 \text{ GeV.}$



Arnold et al 2008

$$lp^\uparrow \rightarrow l\pi^+ X \simeq \Delta^N u \otimes D_{u/\pi^+} > 0$$

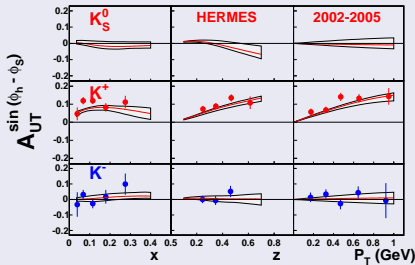
$$lp^\uparrow \rightarrow l\pi^- X \simeq 4\Delta^N u \otimes D_{u/\pi^-} + \Delta^N d \otimes D_{d/\pi^-} \simeq 0$$

$$ID^\uparrow \rightarrow l\pi^+ X \simeq (\Delta^N u + \Delta^N d) \otimes D_{u/\pi^+} \simeq 0$$

HERMES and COMPASS DATA

HERMES

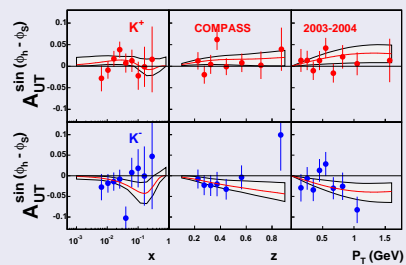
$ep \rightarrow eKX$, $p_{lab} = 27.57$ GeV.



M. Anselmino et al 2009

COMPASS

$\mu D \rightarrow \mu KX$, $p_{lab} = 160$ GeV.



M. Anselmino et al 2009

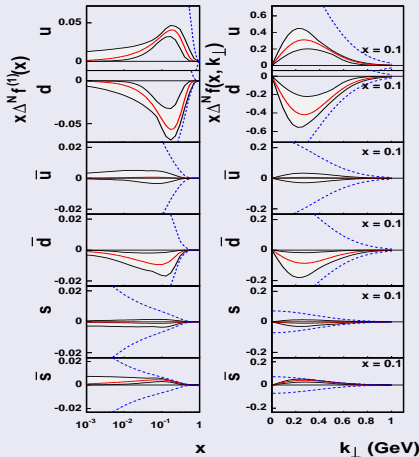
Kaon data allow for light antiquark Sivers function extraction.

M. Anselmino et al 2009

$K^+(u\bar{s})$, $K^-(\bar{u}s)$

Sivers functions

$$\Delta^N f_q^{(1)}(x) \equiv \int d^2 \mathbf{k}_\perp \frac{k_\perp}{4m_p} \Delta^N f_{q/p^\uparrow}(x, k_\perp) = -f_{1T}^{\perp(1)q}(x).$$



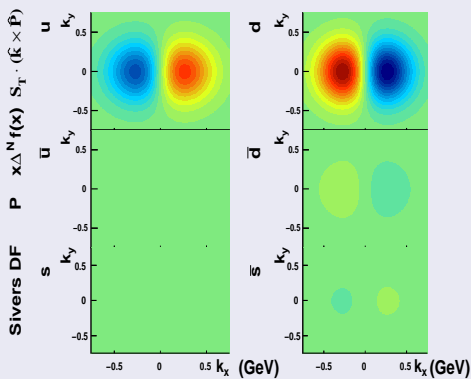
Sivers functions for u , d and *sea* quarks are extracted from **HERMES** and **COMPASS** data.

$\Delta^N f_u > 0$, $\Delta^N f_d < 0$, first hints on nonzero sea quark Sivers functions.

EIC will contribute to flavour separation of Sivers functions.

Three dimensional picture of the proton

The proton moves along $-Z$ direction (into the screen) and S_T is along Y .



Sivers functions for ***u***, ***d*** and ***sea*** quarks are extracted from **HERMES** and **COMPASS** data.

Red color – more quarks.

Blue Color – less quarks.

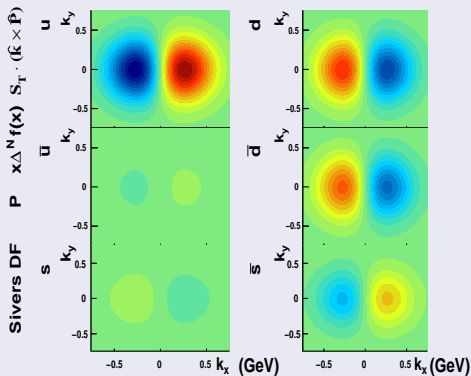
Sivers functions is a left – right asymmetry of quark distribution.

$$x = 0.2$$

No information on sea quarks.

Three dimensional picture of the proton

The proton moves along $-Z$ direction (into the screen) and S_T is along Y .



Sivers functions for *u*, *d* and *sea* quarks are extracted from **HERMES** and **COMPASS** data.

Red color – more quarks.

Blue Color – less quarks.

Sivers functions is a left – right asymmetry of quark distribution.

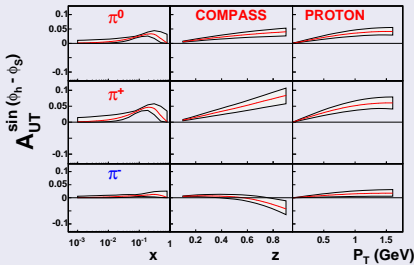
$$x = 0.01$$

More information on sea quarks. EIC will help to separate flavours.

PREDICTIONS

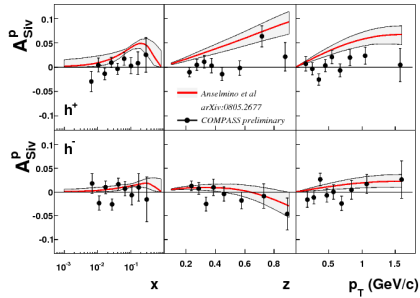
COMPASS on PROTON

$\mu p \rightarrow \mu \pi X$, $p_{lab} = 160$ GeV.



Comparison

preliminary COMPASS data
arXiv:0808.0086



Mismatch of COMPASS and HERMES results on Sivers asymmetry

COMPASS data $\rightarrow Q^2$ dependence of the asymmetry. Not supported by HERMES data. Wider region of Q^2 at fixed x is needed.

Sivers mechanism and Jets @ EIC

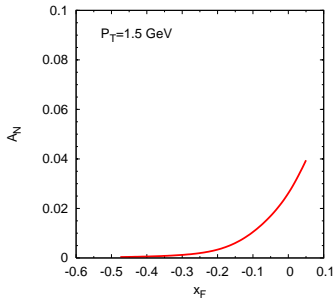
Interesting possibility to study Sivers mechanism via jet production in SIDIS $\gamma^* P \rightarrow Jet X$ allows to study Sivers mechanism

$$A_{UT}^{\sin(\Phi_{jet} - \Phi_S)} \propto \Delta^{N_f} \otimes \sigma$$

pro: no fragmentation function is involved.

cons: cross-section is small, QCD corrections should be accounted for.

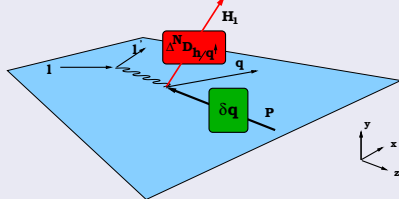
Left-right asymmetry A_N in *lepton* $P \rightarrow Jet X$ can be studied @ EIC



Anselmino et al 09
estimates for EIC
@ $\sqrt{s} = 50$ GeV,
 $p_T = 1.5$ GeV.

Collins effect: SIDIS and e^+e^- annihilation

SIDIS $IN \rightarrow I'H_1X$



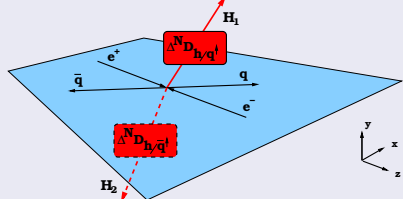
Collins effect gives rise to azimuthal Single Spin Asymmetry

$$\begin{array}{c} \text{Diagram of two quarks with up spin} \\ - \quad \text{Diagram of two quarks with down spin} \\ = \Delta \tau q(x, Q^2) \end{array}$$

$$\begin{array}{c} \text{Diagram of a quark with up spin} \\ - \quad \text{Diagram of a quark with down spin} \\ = \Delta^N D_{h/q^\uparrow}(z, Q^2) \end{array}$$

J. C. Collins, *Nucl. Phys.* **B396** (1993) 161

$e^+e^- \rightarrow H_1H_2X$



Collins effect gives rise to azimuthal asymmetry, q and \bar{q} Collins functions are present in the process:

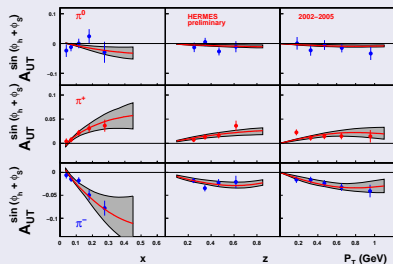
$$\Delta^N D_{h/q^\uparrow}(z_1, Q^2)$$

$$\Delta^N D_{h/\bar{q}^\uparrow}(z_2, Q^2)$$

D. Boer, R. Jacob and P. J. Mulders *Nucl. Phys.* **B504** (1997) 345

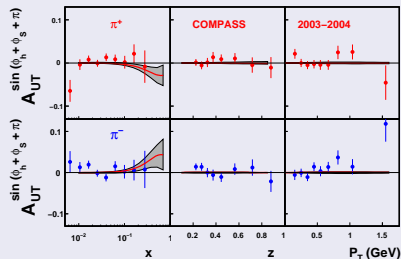
Description of the data

HERMES $A_{UT}^{\sin(\phi_h + \phi_s)}$



$ep \rightarrow e\pi X$, $p_{lab} = 27.57$ GeV.

COMPASS $A_{UT}^{\sin(\phi_h + \phi_s + \pi)}$



$\mu D \rightarrow \mu\pi X$, $p_{lab} = 160$ GeV

M. Anselmino et al., Nucl.Phys.Proc.Suppl.191:98-107, 2009

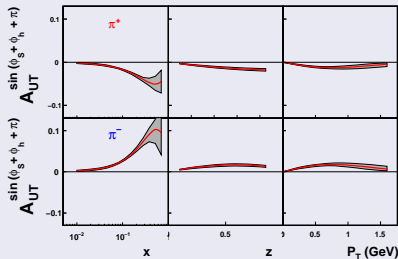
HERMES, M. Diefenthaler, (2007), arXiv:0706.2242

COMPASS, M. Alekseev et al., (2008), Phys.Lett.B673:127-135, 2009

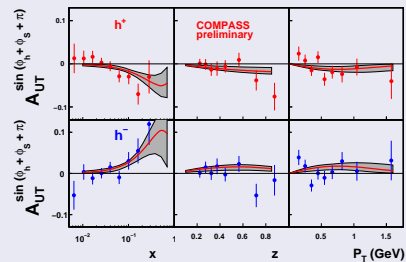
Description of the data

Predictions for COMPASS operating on PROTON target

COMPASS $A_{UT}^{\sin(\phi_h + \phi_s + \pi)}$



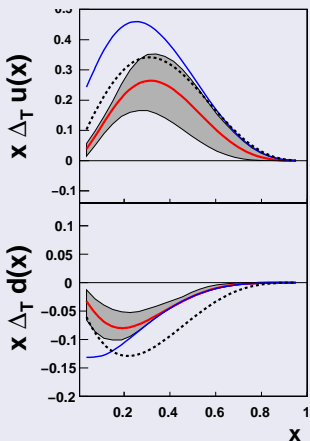
COMPASS $A_{UT}^{\sin(\phi_h + \phi_s + \pi)}$



Comparison with preliminary
COMPASS data arXiv:0808.0086

Anselmino et al 2009

Transversity vs. helicity



- ① Solid red line – transversity distribution

$$\Delta_T q(x)$$

this analysis at $Q^2 = 2.4 \text{ GeV}^2$.

- ② Solid blue line – Soffer bound

$$\frac{q(x) + \Delta q(x)}{2}$$

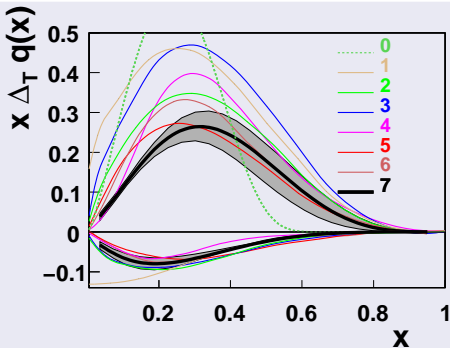
GRV98LO + GRSV98LO

- ③ Dashed line – helicity distribution

$$\Delta q(x)$$

Transversity, comparison with models

New extraction is close to most models.

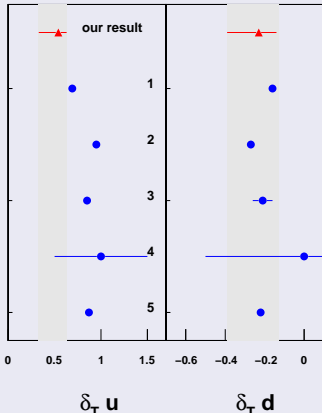


- ① Barone, Calarco, Drago PLB 390 287 (97)
- ② Soffer et al. PRD 65 (02)
- ③ Korotkov et al. EPJC 18 (01)
- ④ Schweitzer et al. PRD 64 (01)
- ⑤ Wakamatsu, PLB B653 (07)
- ⑥ Pasquini et al., PRD 72 (05)
- ⑦ Cloet, Bentz and Thomas PLB 659 (08)
- ⑧ Anselmino et al 2009.

Tensor charges

$$\delta q = \int_0^1 dx (\Delta_T q - \Delta_T \bar{q}) = \int_0^1 dx \Delta_T q$$

$$\Delta_T u = 0.54^{+0.09}_{-0.22}, \Delta_T d = -0.23^{+0.09}_{-0.16} \text{ at } Q^2 = 0.8 \text{ GeV}^2$$



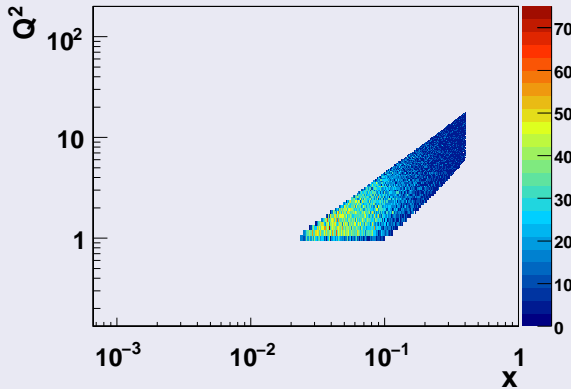
- ➊ Quark-diquark model:
Cloet, Bentz and Thomas
PLB **659**, 214 (2008), $Q^2 = 0.4 \text{ GeV}^2$
- ➋ CQSM:
M. Wakamatsu, PLB **653** (2007) 398.
 $Q^2 = 0.3 \text{ GeV}^2$
- ➌ Lattice QCD:
M. Gockeler et al.,
Phys.Lett.B627:113-123,2005 ,
 $Q^2 = 4 \text{ GeV}^2$
- ➍ QCD sum rules:
Han-xin He, Xiang-Dong Ji,
PRD 52:2960-2963,1995, $Q^2 \sim 1 \text{ GeV}^2$
- ➎ Constituent quark model:
B. Pasquini, M. Pincetti, and
S. Boffi, PRD72(2005)094029 and
PRD76(2007)034020, $Q^2 \sim 0.8 \text{ GeV}^2$

Some snapshots of EIC

EIC will widen kinematical coverage in x and Q^2

HERMES $\sqrt{s} = 7.25$ GeV

Q^2 vs x

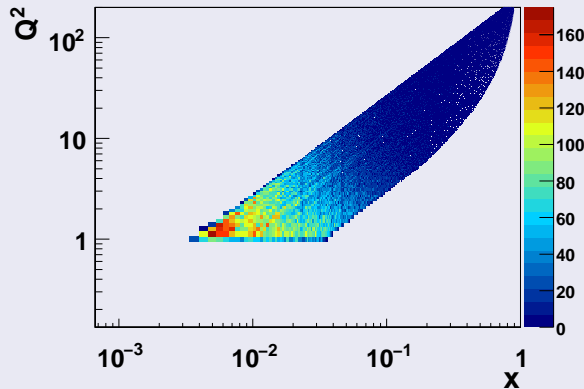


Some snapshots of EIC

EIC will widen kinematical coverage in x and Q^2

COMPASS $\sqrt{s} = 17.32$ GeV

Q^2 vs x

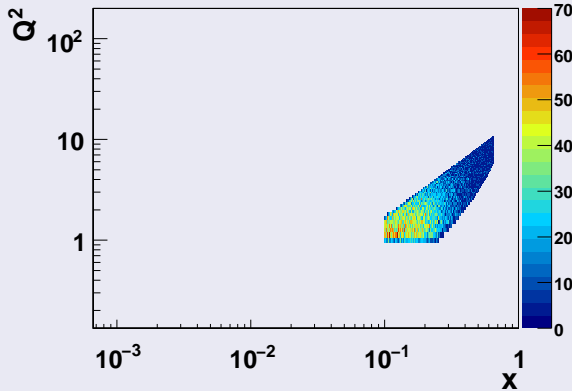


Some snapshots of EIC

EIC will widen kinematical coverage in x and Q^2

JLAB12 $\sqrt{s} = 4.63$ GeV

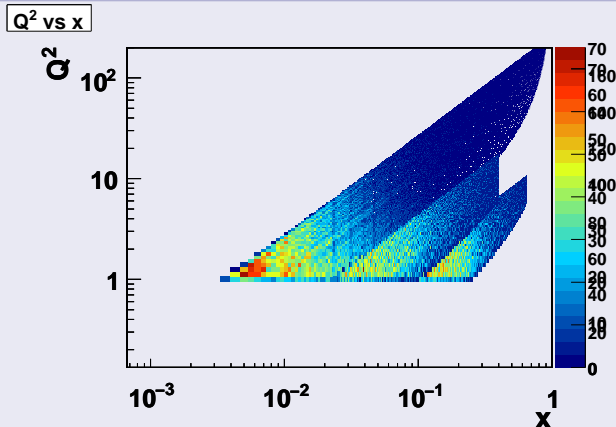
Q^2 vs x



Some snapshots of EIC

EIC will widen kinematical coverage in x and Q^2

JLAB12+HERMES+COMPASS

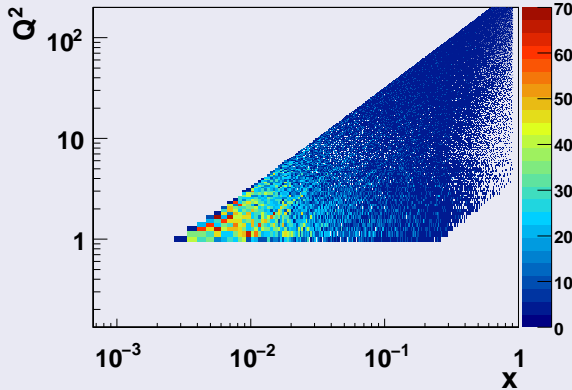


Some snapshots of EIC

EIC will widen kinematical coverage in x and Q^2

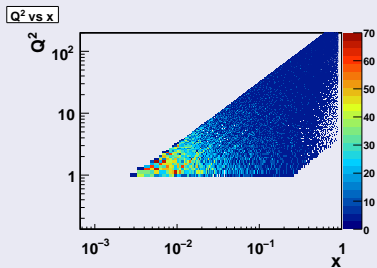
EIC @ $\sqrt{s} = 20$ GeV

Q^2 vs x

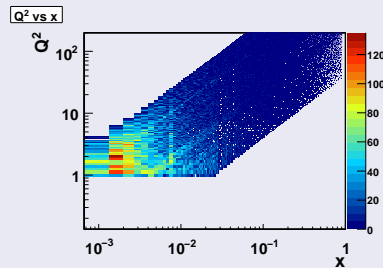


Some snapshots of EIC

EIC @ $\sqrt{s} = 20$ GeV



EIC @ $\sqrt{s} = 65$ GeV



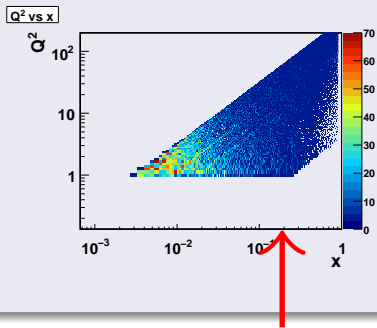
Biggest asymmetries are at $x \sim 0.2$.

Wide range of Q^2 at some fixed x is plausible.

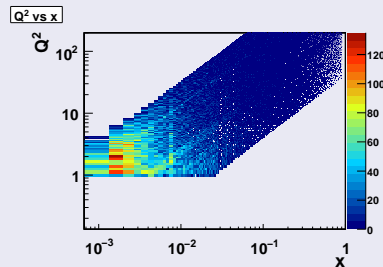
Increasing the energy we go to the low- x region, but loose Q^2 range at moderate x . The energy of the collider should be chosen with great care to accommodate appropriate $x - Q^2$ range.

Some snapshots of EIC

EIC @ $\sqrt{s} = 20$ GeV



EIC @ $\sqrt{s} = 65$ GeV



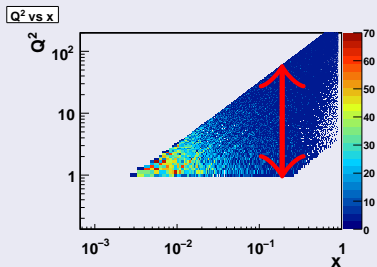
Biggest asymmetries are at $x \sim 0.2$.

Wide range of Q^2 at some fixed x is plausible.

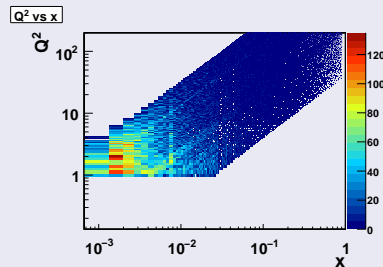
Increasing the energy we go to the low- x region, but loose Q^2 range at moderate x . The energy of the collider should be chosen with great care to accommodate appropriate $x - Q^2$ range.

Some snapshots of EIC

EIC @ $\sqrt{s} = 20$ GeV



EIC @ $\sqrt{s} = 65$ GeV



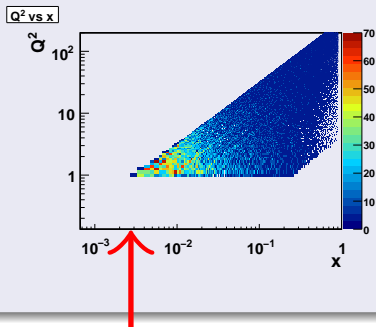
Biggest asymmetries are at $x \sim 0.2$.

Wide range of Q^2 at some fixed x is plausible.

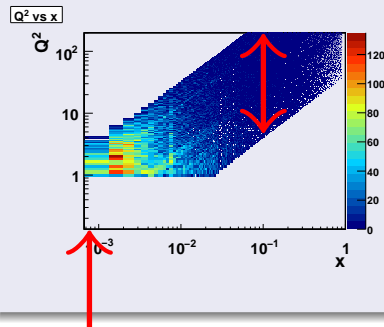
Increasing the energy we go to the low- x region, but loose Q^2 range at moderate x . The energy of the collider should be chosen with great care to accommodate appropriate $x - Q^2$ range.

Some snapshots of EIC

EIC @ $\sqrt{s} = 20$ GeV



EIC @ $\sqrt{s} = 65$ GeV



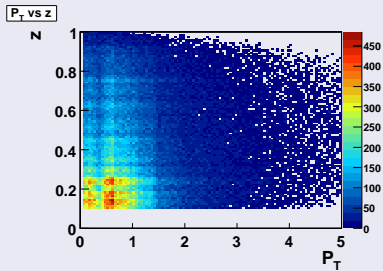
Biggest asymmetries are at $x \sim 0.2$.

Wide range of Q^2 at some fixed x is plausible.

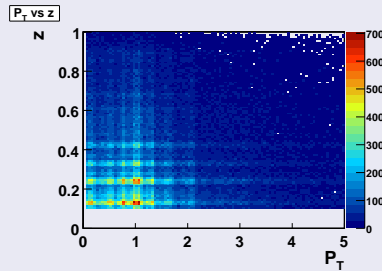
Increasing the energy we go to the low- x region, but loose Q^2 range at moderate x . The energy of the collider should be chosen with great care to accommodate appropriate $x - Q^2$ range.

Some snapshots of EIC

EIC @ $\sqrt{s} = 20$ GeV



EIC @ $\sqrt{s} = 65$ GeV

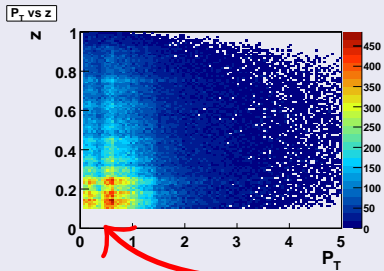


High P_T range allows to test intermediate region where both TMD and collinear factorizations are valid.

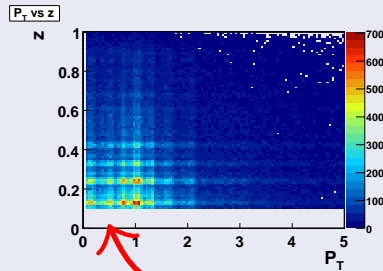
In these estimates only non perturbative TMD cross sections were used. Actual distributions will be shifted towards higher P_T .

Some snapshots of EIC

EIC @ $\sqrt{s} = 20$ GeV



EIC @ $\sqrt{s} = 65$ GeV

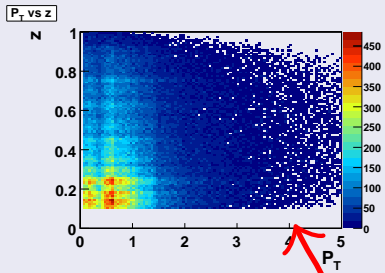


High P_T range allows to test intermediate region where both TMD and collinear factorizations are valid.

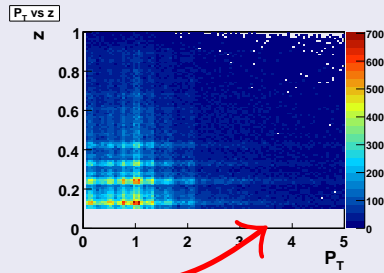
In these estimates only non perturbative TMD cross sections were used. Actual distributions will be shifted towards higher P_T .

Some snapshots of EIC

EIC @ $\sqrt{s} = 20$ GeV



EIC @ $\sqrt{s} = 65$ GeV

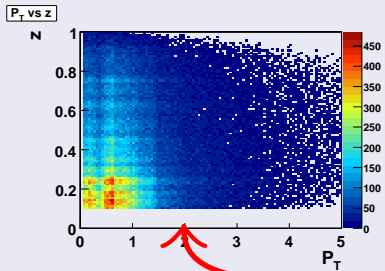


High P_T range allows to test intermediate region where both TMD and collinear factorizations are valid.

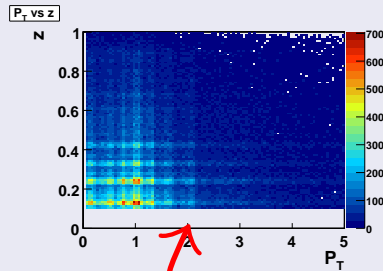
In these estimates only non perturbative TMD cross sections were used. Actual distributions will be shifted towards higher P_T .

Some snapshots of EIC

EIC @ $\sqrt{s} = 20$ GeV



EIC @ $\sqrt{s} = 65$ GeV



High P_T range allows to test intermediate region where both TMD and collinear factorizations are valid.

In these estimates only non perturbative TMD cross sections were used. Actual distributions will be shifted towards higher P_T .

CONCLUSIONS

- EIC will be a powerful tool to study parton dynamics and TMDs.
- High Q^2 range will allow to study twist-2 functions and higher twist content of the nucleon.
- Range of P_T will allow to study intermediate region where both TMD and collinear factorizations are applicable.
- Q^2 range at some fixed x will provide information on Q^2 behaviour of the asymmetries and Q^2 evolution of TMDs.
- Full flavour and spin decomposition of TMDs can be attempted at EIC.

CONCLUSIONS

- EIC will be a powerful tool to study parton dynamics and TMDs.
- High Q^2 range will allow to study **twist-2** functions and higher twist content of the nucleon.
- Range of P_T will allow to study intermediate region where both TMD and collinear factorizations are applicable.
- Q^2 range at some fixed x will provide information on Q^2 behaviour of the asymmetries and Q^2 evolution of TMDs.
- Full flavour and spin decomposition of TMDs can be attempted at EIC.

CONCLUSIONS

- EIC will be a powerful tool to study parton dynamics and TMDs.
- High Q^2 range will allow to study **twist-2** functions and higher twist content of the nucleon.
- Range of P_T will allow to study intermediate region where both TMD and collinear factorizations are applicable.
- Q^2 range at some fixed x will provide information on Q^2 behaviour of the asymmetries and Q^2 evolution of TMDs.
- Full flavour and spin decomposition of TMDs can be attempted at EIC.

CONCLUSIONS

- EIC will be a powerful tool to study parton dynamics and TMDs.
- High Q^2 range will allow to study **twist-2** functions and higher twist content of the nucleon.
- Range of P_T will allow to study intermediate region where both TMD and collinear factorizations are applicable.
- Q^2 range at some fixed x will provide information on Q^2 behaviour of the asymmetries and Q^2 evolution of TMDs.
- Full flavour and spin decomposition of TMDs can be attempted at EIC.

CONCLUSIONS

- EIC will be a powerful tool to study parton dynamics and TMDs.
- High Q^2 range will allow to study **twist-2** functions and higher twist content of the nucleon.
- Range of P_T will allow to study intermediate region where both TMD and collinear factorizations are applicable.
- Q^2 range at some fixed x will provide information on Q^2 behaviour of the asymmetries and Q^2 evolution of TMDs.
- Full flavour and spin decomposition of TMDs can be attempted at EIC.

CONCLUSIONS

- EIC will be a powerful tool to study parton dynamics and TMDs.

THANK YOU!

- Range of P_T will allow to study intermediate region where both TMD and collinear factorizations are applicable.
- Q^2 range at some fixed x will provide information on Q^2 behaviour of the asymmetries and Q^2 evolution of TMDs.
- Full flavour and spin decomposition of TMDs can be attempted at EIC.